frontiers | Frontiers in Earth Science

ORIGINAL RESEARCH
published: 07 April 2022
doi: 10.3389/feart.2022.845924

Anisotropy of Magnetic Susceptibility Reveals Late Miocene Tectonic Activity in the Western Qaidam Basin

Weilin Zhang[1,2]*, *Bingshuai Li*[3] and *Maodu Yan*[1,2]

[1]State Key Laboratory of Tibetan Plateau Earth System, Resources and Environment, Institute of Tibetan Plateau Research (TPESRE), Chinese Academy of Sciences, Beijing, China, [2]Key Laboratory of Continental Collision and Plateau Uplift, Institute of Tibetan Plateau Research, Chinese Academy of Sciences, Beijing, China, [3]School of Earth Sciences, East China University of Technology, Nanchang, China

The western Qaidam Basin on the northeastern Tibetan Plateau located at the intersection between the Altyn Tagh Fault and the Kunlun Fault/Qimen Tagh Fault holds significant potential to reveal the tectonic process of these two faults as well as the evolution of the Qaidam Basin. In this paper, we conducted detailed anisotropy of magnetic susceptibility (AMS) records from Late Cenozoic sediments at the Qigequan section in the western Qaidam Basin to shed new light on the tectonic processes in this region. Based on the distribution of three principal axes of magnetic fabrics as well as magnetic fabric parameters, the AMS records can be divided into three parts. The lower part (~6.9–4.6 Ma), mainly made of fine-grained mudstone and siltstone, exhibits three well-grouped principal axes with a NE-SW elongated K_{min} axis as the embryonic tectonic magnetic fabric, suggesting constant NE-SW compressional strain. The middle part (~4.6–3.0 Ma), characterized by mudstone, siltstone and sandstone, shows three less grouped principal axes and suggests a relatively weak and stable tectonic environment. The three principal axes of the upper part (~2.4–0.4 Ma) is composed of sandstone and conglomerate of the Qigequan Formation, similar to the middle part, which was primarily attributed to the coarse lithology and not sensitive to tectonics since ~2.6 Ma. The NE-SW compressional strain in the western Qaidam Basin is consistent with that in the northeastern basin, both of which are parallel to the upper crust movements revealed by the GPS, suggesting the dominant NE-SW compressional strain in the western and northern basins in the late Cenozoic. The decreasing magnitude of tectonic activities during ~6.9–4.6 Ma indicates that the major geological units released most of the compressional strain in the western Qaidam Basin during tectonic activity that initiated in the early-late Miocene.

Keywords: anisotropy of magnetic susceptibility, northeastern Tibetan Plateau, Qaidam Basin, Qigequan, late Cenozoic, magnetic fabric

OPEN ACCESS

Edited by:
Yunfa Miao, Northwest Institute of Eco-Environment and Resources (CAS), China

Reviewed by:
Zhiming Sun, Chinese Academy of Geological Sciences (CAGS), China
Renata Nela Tomezzoli, Consejo Nacional de Investigaciones Científicas y Técnicas (CONICET), Argentina

***Correspondence:**
Weilin Zhang
zhangwl@itpcas.ac.cn

Specialty section:
This article was submitted to Structural Geology and Tectonics, a section of the journal Frontiers in Earth Science

Received: *30 December 2021*
Accepted: *11 February 2022*
Published: *07 April 2022*

Citation:
Zhang W, Li B and Yan M (2022) Anisotropy of Magnetic Susceptibility Reveals Late Miocene Tectonic Activity in the Western Qaidam Basin. Front. Earth Sci. 10:845924. doi: 10.3389/feart.2022.845924

1 INTRODUCTION

The Cenozoic India-Eurasia collision is the most prominent tectonic event that not only dominates the basic geological framework in the Tibetan Plateau (Tapponnier and Molnar, 1977; Yin and Harrison, 2000) but also generates large far-field effects on the tectonic deformations of the other regions of the Asian continent (Yin et al., 1998; Holt et al., 2000; Chen et al., 2017; Tian et al., 2021). The interior basins in the Tibetan Plateau with thick Cenozoic sediments archive key information on

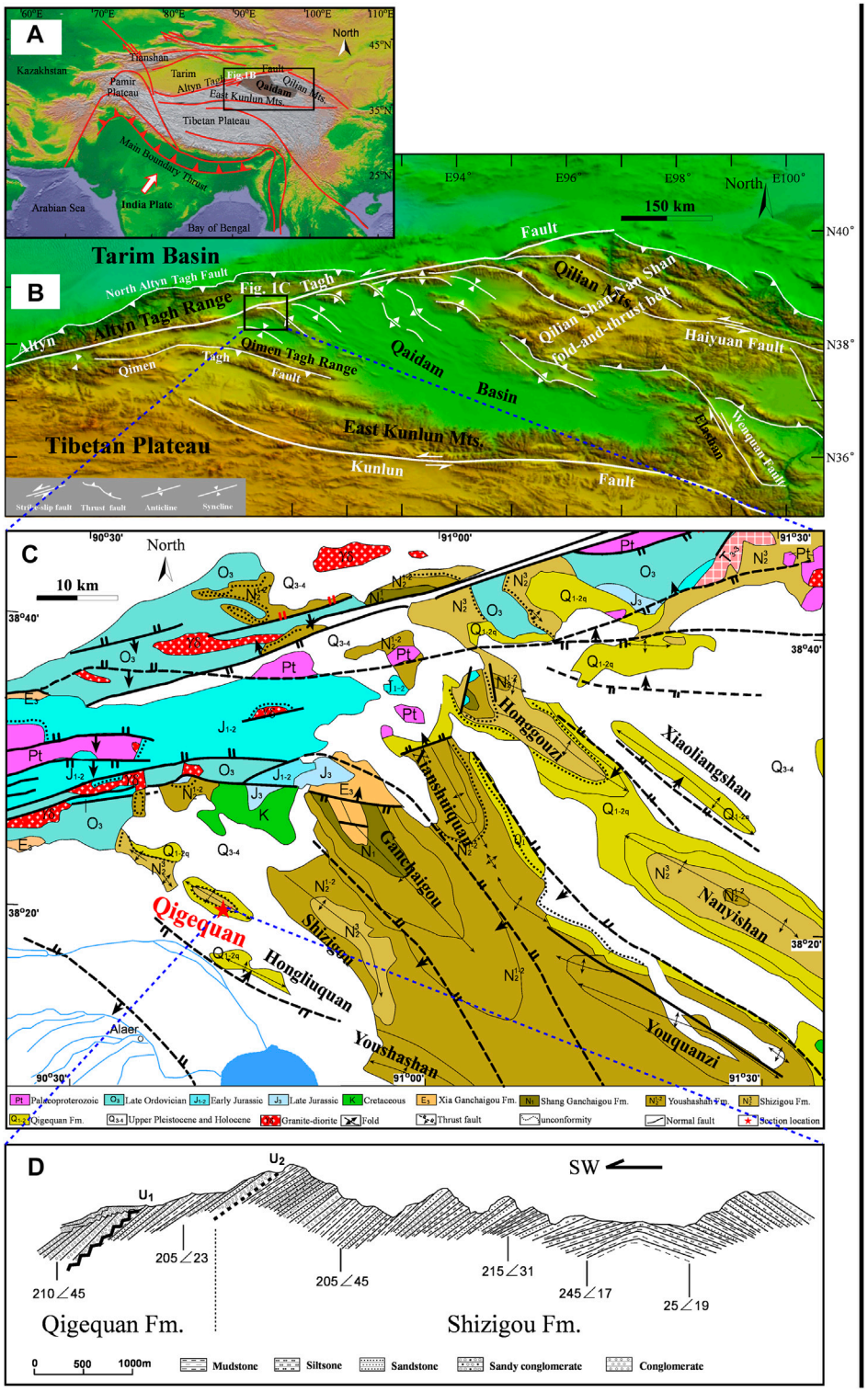

FIGURE 1 | (A) Tectonic digital elevation model (DEM) map of the Tibetan Plateau and it adjacent regions showing the major thrust faults [modified from Sun J. et al. (2005)]. **(B)** DEM map of the northeastern region of the NE Tibetan Plateau showing the locations of the Qaidam Basin [modified from Li et al. (2017)]. See Panel **(A)** for its geological area. **(C)** Geological map of the western Qaidam Basin showing the location of the Qigequan profile (red pentagram). See Panel **(B)** for its location in the Qaidam Basin. **(D)** Cross-section along the Qigequan section. **(B,C)** are modified from Zhang et al. (2013).

the tectonic deformation and uplift process of the plateau (Fang et al., 2007, Wang et al., 2008; Chen et al., 2020; Zhang et al., 2020a; Fang et al., 2020b), as well as paleoclimate change (e.g., Fang et al., 2020a; Xiong et al., 2020).

The Qaidam Basin is the largest intermountain basin in the northeastern (NE) Tibetan Plateau, where almost successive Cenozoic sediments were deposited (**Figures 1A,B**). The western Qaidam Basin is located in the triangular zone between the Altyn Tagh Range, Qimen Tagh and Qaidam Basin. It is the key region that holds significant potential in revealing the mountain building history, thrusting and strike-slip faulting of surrounding mountains and faults (Yin et al., 2008; Zhang et al., 2016; Li et al., 2017; Li et al., 2018). To date, tectonic activity records in the western Qaidam Basin have mainly been revealed by mountain buildings or rapid cooling events from thermochronology (Jolivet et al., 2001; Wang et al., 2006; Wang et al., 2008; Liu et al., 2017), growth strata revealed by seismic reflection profiles or through detailed fieldwork analysis (Wang et al., 2012; Cheng et al., 2014; Li et al., 2017; Liu et al., 2019), and abrupt changes in lithology, sedimentation rates and magnetic susceptibility (Chang et al., 2015; Zhang et al., 2016). However, tectonic strain, which is the ultimate factor controlling mountain building, thrusting and strike-slip faulting, is largely ignored, inducing a poor understanding of tectonic deformation of the basin and its surrounding mountains.

Tectonic strain can be traced by many proxies in foreland sediments, such as the strikes of beddings, faults and mountains, orientations of folding axes, and joints (Pueyo et al., 2012 and references therein). Among them, the low-field anisotropy of magnetic susceptibility (AMS) is the most reliable and sensitive strain indicator (Parés et al., 1999; Soto et al., 2009). Li et al. (2008) first reported AMS results from the Xiaganchaigou to Shizigou Formations (Fm) in the northwest part of the Youshashan anticline and suggested that these magnetic fabrics were mainly primary sedimentary magnetic fabrics with NE-ward compressional strain. This is consistent with a later study by Yu et al. (2014) that is based on the AMS records from the Xiaganchaigou and Xiayoushashan Fms from the Huatugou and Gansen sections. However, these AMS studies were mainly conducted by section-based (Li et al., 2008) or site-based sampling (Yu et al., 2014), which may be insufficient to reveal or average out the detailed strain variations in this region (Li et al., 2020; Li et al., 2021). In addition, the age of these two AMS records was dated mostly before the middle Miocene. Thus, successive AMS records, especially after the middle Miocene, are needed in the western Qaidam Basin to trace the variations in tectonic strain and depositional conditions.

In this study, we conducted a detailed AMS study along an ~800-m-thick Qigequan profile in the western Qaidam Basin to decipher the post-Late Miocene deformation process in this region.

2 GEOLOGICAL SETTING

The Qaidam Basin in the NE Tibetan Plateau has a relatively low subsidence (~2,800–3,000 m) compared to the large surrounding mountains (>4,000 m), i.e., the Qilian Shan to the northeast, the Altyn Tagh Range to the northwest, the Qimen Tagh Range and East Kunlun Mountain to the south and southwest, and the Ela Shan to the east (**Figure 1B**). Nearly successive Cenozoic lacustrine-fluvial sediments were deposited and provided as an ideal place to reveal the tectonic deformation and uplift process of the Tibetan Plateau as well as the climate changes (e.g., Yin and Harrison, 2000; Yin et al., 2002; Fang et al., 2019). Seven Fms were divided and can be correlated throughout the basin; in ascending order they are: the Lulehe Fm, the Xiaganchaigou Fm, the Shangganchaigou Fm, the Xiayoushashan Fm, the Shangyoushashan Fm, the Shizigou Fm and the Qigequan Fm. Their ages have been defined based on dense networks of seismic reflection profiles, fossil assemblages and magnetostratigraphic studies (Qinghai, 1991; Sun Z. et al., 2005; Fang et al., 2007; Lu and Xiong, 2009; Song et al., 2014; Chang et al., 2015; Ji et al., 2017; Wang et al., 2017; Fang et al., 2019; Nie et al., 2019). However, two age models have been proposed based on fossil assemblages and magnetostratigraphic studies in the northern Qaidam Basin. The traditional interpretation prefers an older age model that believed that deposition of the Cenozoic sediments was initiated since the early Cenozoic (Paleocene to early Eocene) not long after the India-Asia collision (i.e., Yin et al., 2008; Ji et al., 2017), while the recent emerging younger age model argued that Cenozoic deposition initiated quite late since the late Oligocene or early Miocene (Wang et al., 2017; Nie et al., 2019). Further studies based on definite fossils and volcanic ash in the lower part of the sediments are required to clarify these contrasting viewpoints. Another point should also be noted that these two contrasting age models were mainly based on magnetostratigraphic studies in the northern Qaidam Basin. However, the western Qaidam Basin is quite different in that the oldest exposed Cenozoic sediments are the upper Xiaganchaigou Fm, and magnetostratigraphic studies are generally consistent with each other (Zhang et al., 2012; Zhang et al., 2013; Song et al., 2014; Chang et al., 2015). In addition, a recent study that balanced the sediments preserved in the basin with materials eroded in the drainage area also preferred the traditional age model in the western Qaidam Basin (Cheng et al., 2018). Thus, the traditional ages of formations in the western Qaidam Basin are compatible with geological events.

The western Qaidam Basin is the intersection area between the Altyn Tagh Fault (ATF) and the Kunlun/Qimen Tagh Fault (**Figure 1B**). A series of NW-SE trending echelon folds and fault shapes the geomorphological features in this area. The Qigequan anticline is a brachy anticline developed with a NW-SE trending axis in the western Qaidam Basin. It is parallel to the Youshashan anticline in its western part, as the latter is the largest en echelon anticline in the western Qaidam Basin (**Figure 1C**). Over 800 m of late Cenozoic sediments, which include the Shizigou and the Qigequan Fm, were exposed along the southern limb of the anticline (**Figure 1D**). The Shizigou Fm is ~501 m thick and is mainly dominated by mudstone, siltstone and sandstone that were deposited mainly under a lacustrine or fan-delta environment. The Qigequan Fm is ~304 m thick and is disconformably (U_2) overlying the lower Shizigou Fm and characterized by sandstone, sandy conglomerate and

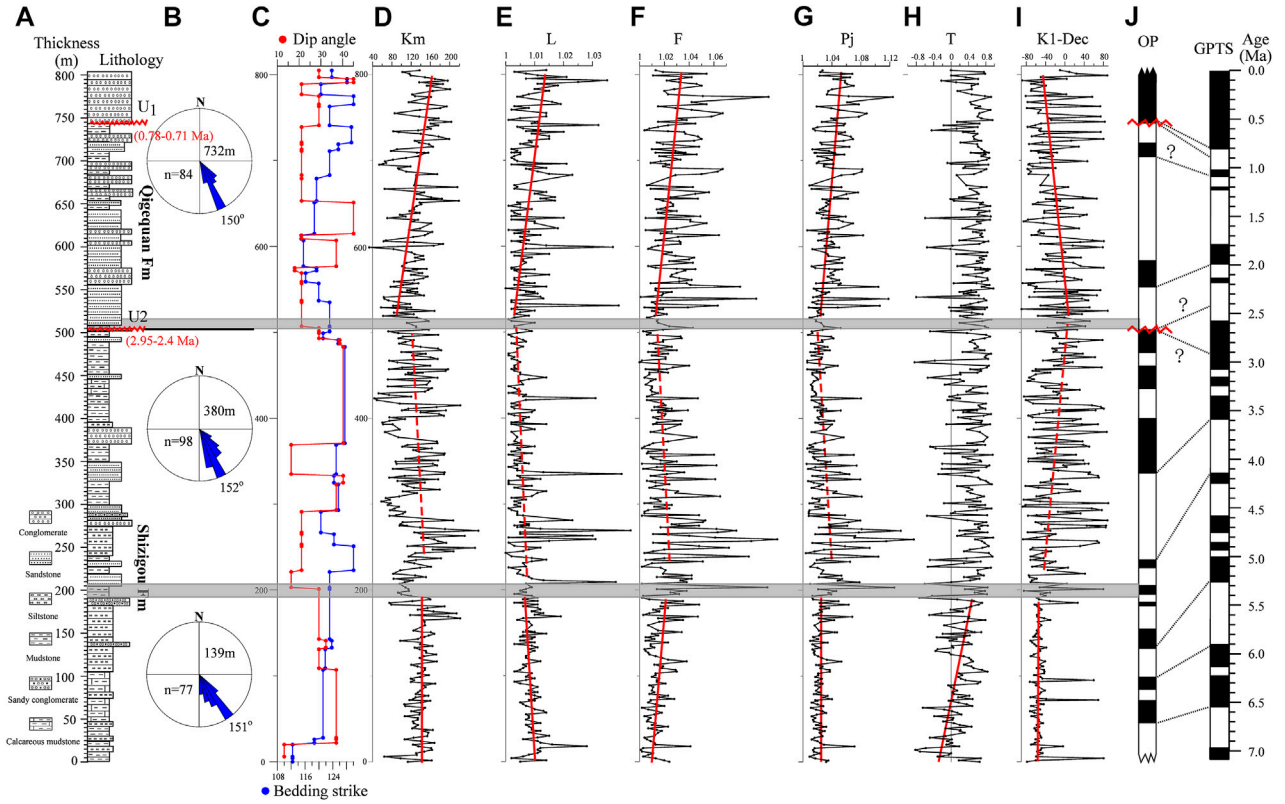

FIGURE 2 | Lithostratigraphy **(A)**, restored paleocurrent directions **(B)**, bedding strike and dip **(C)**, AMS parameters (magnetic susceptibility (Km), lineation (L), foliation (F), corrected degree of anisotropy (Pj), shape parameter (T) and declination of K_1 in tilt corrected coordinates) **(D–I)** and polarity correlations with the geomagnetic polarity time scale **(J)** plotted against depth in the Qigequan profile (Zhang et al., 2013).

conglomerate that were deposited mainly under a fan delta or fluvial environment. In addition, another disconformity (U_1) exists in the upper part of the Qigequan Fm. (**Figure 1D**). The lithology of the whole profile exhibits an upward coarsening trend, which is mostly attributed to the intensive tectonic deformations in this region (Wang et al., 2012; Bao et al., 2017). Detailed magnetostratigraphic studies have been performed along the Qigequan profile and have constrained these Late Neogene sedimentary sequences to ~6.9–0.4 Ma, with two unconformities being ~2.95–2.4 Ma and ~0.78–0.71 Ma, respectively (**Figures 2A,J**) (Zhang et al., 2013).

3 PALEOMAGNETIC SAMPLING AND MEASUREMENTS

Block samples were collected mainly from mudstone, siltstone and sandstone with a mean sampling interval of 2–3 m that ranged depending on the lithology. In total, 408 samples were collected along the Qigequan profile (Zhang et al., 2013). For further magnetic fabric and demagnetization procedures, all samples were cut into standard cubic specimens with a 2.0 cm edge length in the laboratory for further thermal demagnetization, rock magnetic and AMS procedures. In addition, to decipher the possible relations between the magnetic lineations and hydraulic conditions, clast imbrications in conglomerates were measured at three sites (~139 m, 380 and 732 m) with more than 70 pebble imbrications at each site along the profile to restore the paleocurrent directions (**Figure 2B**).

AMS has been suggested to be a rapid and sensitive method to reveal the preferred orientation of magnetic grains, which is closely related to depositional and/or tectonic regimes (Parés et al., 1999; Soto et al., 2009; Sun et al., 2016; Li et al., 2020). It can be geometrically illustrated as a triaxial ellipsoid with three principal axis directions: the maximum (K_{max} or K_1), intermediate (K_{int} or K_2) and minimum (K_{min} or K_3). The corrected degree of anisotropy (Pj) is generally sensitive to lithological changes (e.g., the clay content) and strain (Hrouda, 1982), the shape parameter (T) describes the shape of the degree of anisotropy as a negative value ($-1 < T < 0$) corresponding to a prolate (i.e., rod-shaped) ellipsoid, and a positive value ($0 < T < 1$) corresponding to an oblate (i.e., disk-shaped) ellipsoid (Hrouda, 1982; Tarling and Hrouda, 1993). All these parameters can be automatically calculated by the Anisoft 42 software developed by Martin and Jelinek (2009).

The AMS of all specimens was measured using a KLY-3CS3 Kappabridge (AGICO) with an automated sample rotating system under an applied field of 423 A/m at a low frequency

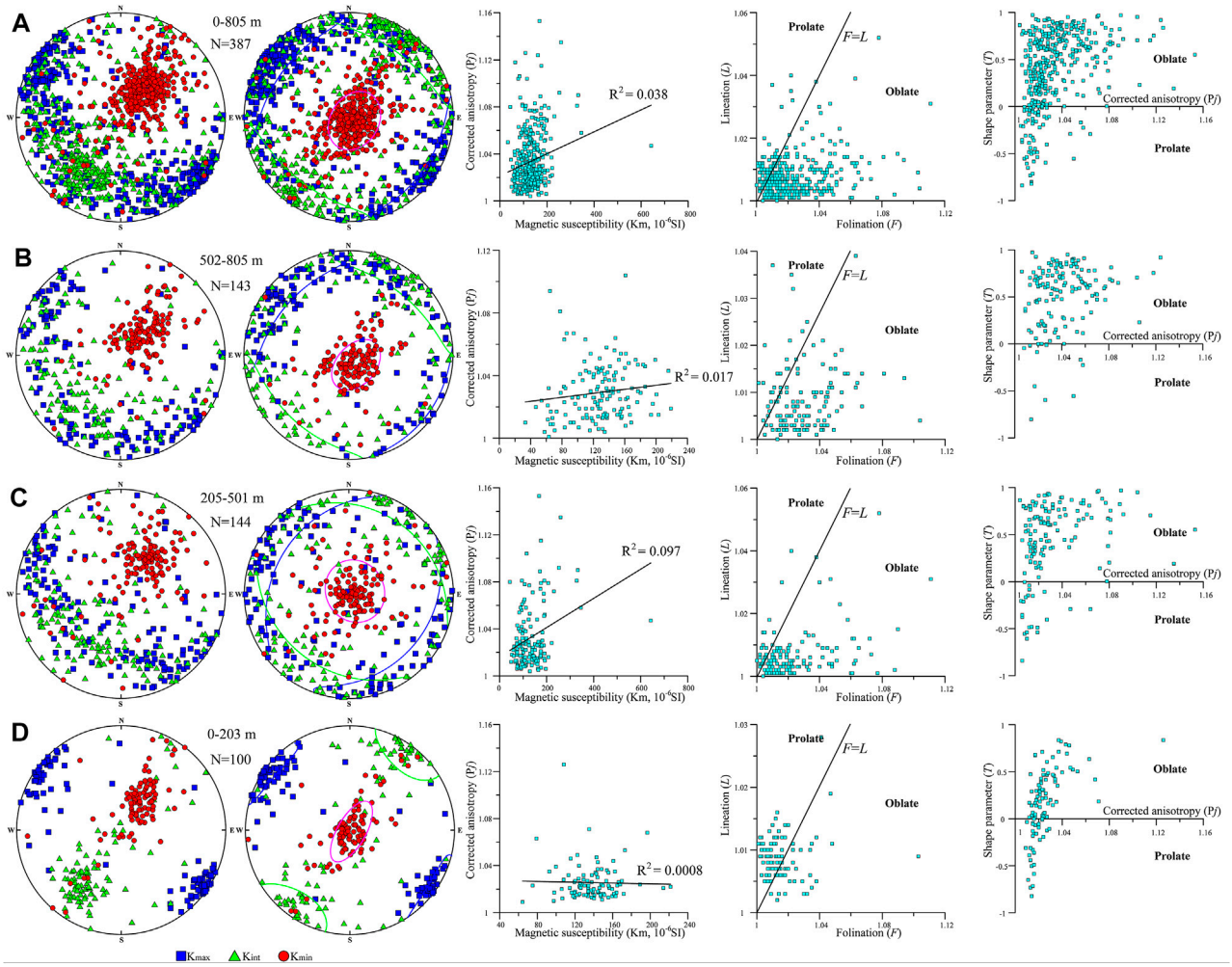

FIGURE 3 | AMS results including equal-area stereographic projections of the AMS principal axes in both *in situ* and bedding-corrected coordinates (squares, triangles and circles represent K_{max}, K_{int}, and K_{min} axes, respectively), the mean magnetic susceptibility (Km) versus corrected anisotropy (Pj), foliation (F) versus lineation (L) plots, and Pj-T diagrams) of the total samples **(A)**, samples from 502 to 805 m **(B)**, samples from 205 to 501 m **(C)** and samples from 0–203 m **(D)** along the Qigequan profile.

of 875 Hz at the Center for Applied Geoscience, Tübingen University.

4 RESULTS

4.1 Restored Paleocurrent Directions

The restored paleocurrent directions from pebble imbrications in the Qigequan anticline region were relatively stable with a WSW-ward direction (~150°) since the deposition of the Shizigou Fm (**Figure 2B**). This result is consistent with previous results from the Xichagou or Huatugou section ~20 km to the northwest of the Qigequan section, with south/southwestward paleocurrents or north/northwestward provenance by analyzing conglomerate imbrications, cross stratifications and heavy mineral assemblages (Wu et al., 2012; Li et al., 2015). These results indicate that the provenance of detrital grains in the Qigequan region was consistent with the Altyn Tagh Range in the north since the Late Miocene. However, it could not be ruled out that the Qilian mountains and East Kunlun mountains had not provided the sediments for the other deposited regions in the western of Qaidam Basin.

4.2 Anisotropy of Magnetic Susceptibility Results

Previous rock magnetic experiments (isothermal remanent magnetization (IRM) acquisition and back field demagnetization curves) and thermal demagnetization behaviors indicate that magnetite and hematite are the main magnetic carriers for these samples (Zhang et al., 2013), as are those for the magnetic susceptibilities.

The bulk magnetic susceptibility (Km) and magnetic fabric parameters exhibit obvious changes along the Qigequan

stratigraphic depth (**Figures 2D–I**). The Km ranges from ~33.14 to 259 μSI with an average value of 133 ± 49 μSI. It was very stable in the lower part (0–203 m), quite variable in the middle part (205–501 m) and exhibited an increasing trend in the upper part (~502–805 m) (**Figure 2D**). A similar change is also observed for the magnetic lineation (L), magnetic foliation (F) and corrected degree of anisotropy (Pj) in the middle and upper parts (**Figures 2E–G**), suggesting that L, F and Pj are possibly related to the mineralogy during these periods. However, the Pj and Km diagrams indicate poor correlations between these two factors (**Figure 3**), suggesting that Pj has no direct relation with lithology. L and F exhibit the opposite behavior in the lower part (**Figures 2E,F**), both of which are independent of Km (**Figure 3**), suggesting that these two parameters are independent of the lithology in the lower part. The T for most samples was positive with an oblate magnetic fabric (**Figure 2H**), suggesting the dominant compaction process during deposition. Nevertheless, the T has a quite different variation, that it shows an increasing trend from prolate to oblate in the lower part, while relatively constant in the middle and upper part, suggesting T variation is independent of mineralogy. The variation of magnetic lineation (K_{max}-Dec) orientations has a negative correlation with that of bedding strike that it exhibits a seemingly clockwise rotation trend from NW-SE (−45°) in the lower part to nearly N-S (0°) in the middle part, and again turn to NW-SE (−45°) with a counterclockwise rotation trend in the upper part.

For the three principal axes of the AMS ellipsoids tilt-corrected on the equal-area stereographic projections, the K_{max} axes are grouped with a low mean inclination (Dec = 307.0°, Inc = 5.4°) and parallel to the bedding strike or fold axis in a NW-SE direction (**Figure 3**). The K_{min} axes are grouped around the bedding pole with a slight NE-SW girdle distribution, which is nearly perpendicular to the bedding strike or the fold axis. These distribution features are commonly observed in foreland basin sediments and are mostly attributed to the layer parallel shortening (LPS) process during deposition (Huang et al., 2006; Charreau et al., 2009; Tang et al., 2012; Yu et al., 2014; Tang et al., 2015; Li et al., 2020).

Based on variations in magnetic fabric parameters, the AMS ellipsoids can also be correspondingly divided into three parts: the lower (0–203 m), middle (205–501 m) and upper (502–805 m) parts (**Figure 3**). For the lower part, the three principal axes were separated from each other, and the magnetic lineations were well developed in a NW-SE direction. The K_{min} and K_{int} axes exhibited an obvious NE-SW girdle distribution that gives rise to typically triaxial to prolate ellipsoids (**Figure 3D**). For the middle and upper parts, the K_{max} and K_{int} axes were not well separated from each other (**Figures 3B,C**). Thus, the magnetic lineations were not well developed compared to the lower part. Despite this, the preferred orientation for the magnetic lineation still has a NW-SE direction. The K_{min} axes were well clustered around the bedding pole, which is more "composite sedimentary/tectonic" fabric in terms of Weil and Yonkee, 2009 instead of a pure sedimentary fabric, since the axis K_{max} is tectonically aligned and parallel to the axis of the folds.

5 DISCUSSION

5.1 Origin of Magnetic Fabrics

The magnetic susceptibility (Km) along the Qigequan profile seems closely related to the lithology (**Figures 2A,D**). The Km in the lower part is quite stable for mainly fine-grained mudstone and siltstone that were deposited under a stable lacustrine environment. For the middle part, the Km has a good correlation with the fine-grained mudstone/siltstone and coarse-grained sandstone/sandy conglomerate sedimentary cycle deposited under a lacustrine or fan-delta environment. The Km has an increasing trend from the center of the sequence to upwards (**Figure 2D**), which is in accordance with the upward coarsening sequence. Recent studies of rock magnetism have proposed that magnetic susceptibility variations are closely related to climate and/or source region changes (Thompson et al., 1980; Sun J. et al., 2005; Zhang et al., 2016). Thus, this increasing trend of Km in the middle part could be attributed to climate-controlled pedogenic processes, which could form new magnetic minerals (Zhou et al., 1990; Maher and Thompson, 1992), and/or changes in source materials (Sun J. et al., 2005; Zhang et al., 2016). Together with the coarse-grained lithology and intensive tectonic deformations during the Quaternary (Zhang et al., 2013; Wei et al., 2016; Bao et al., 2017), we prefer the changes of source materials that called the active tectonics model to interpret this increasing trend of the Km, which has been previously proposed by Sun J. et al. (2005) and Zhang et al. (2016) in the Tiejianggou and Honggouzi sections along the ATF to interpret the relatively high Km since ~13.7 Ma and ~10 Ma, respectively. This model indicates that intensive tectonics result in uplift and exposure of new bedrock that is relatively rich in magnetite and is transported to the depositional region by relatively high-energy currents with a short distance from the source to sink compared to the past.

The AMS has been proven to be a useful tool to trace magma flow directions (Macdonald and Palmer, 1990; Borradaile and Henry, 1997), paleocurrent or wind directions (Zhang et al., 2010; Sun et al., 2016) and compressional or extensional strains, even in weakly deformed foreland sediments without visible deformed features (Parés et al., 1999; Soto et al., 2009; Tang et al., 2012; Li et al., 2020). For the Cenozoic magnetic fabrics in the Qaidam Basin, some studies proposed that they were mainly attributed to tectonism and thus used to indicate compressional strain direction variations from nearly N-S to NE-SW, although the transition time is still under debate (Li et al., 2008; Yu et al., 2014; Su et al., 2016; Li et al., 2020). Other studies argued that these magnetic fabrics, especially since the Xiaganchaigou Fm., were mainly hydraulic force-induced fabrics that were either strong (Nie et al., 2019) or weak currents (Huo et al., 2020) and further applied to reflect basin rotations. Thus, different attributes of magnetic fabrics can lead to distinct tectonic implications. For the magnetic fabrics along the Qigequan profile, it is necessary to

decipher what geological processes shaped these characteristics of magnetic fabrics.

Since the Shizigou and Qigequan Fms have quite similar bedding attitudes (**Figures 1D**, **2C**), the Qigequan anticline is mostly formed after the deposition of the Qigequan Fm (~0.4 Ma). Because the decline in K_{max} has a negative correlation with the bedding strikes, the magnetic lineations along the Qigequan profile were unlikely to be related to the latter tectonic deformation that resulted in the Qigequan anticline. Used together with the quite young geological age of these sediments (since the Late Miocene), different distributions of three principal axes and the varied magnetic fabric parameters along the profile (**Figures 2**, **3**), the magnetic fabric results were mostly the primary magnetic fabrics that acquired during or not long after the deposition and can be attributed to the hydraulic force or tectonic process, despite that the original magnetic fabrics can also be overprinted by the later-stage more intensive deformations (Larrasoaña et al., 2004; Soto et al., 2009; Larrasoaña et al., 2011).

For magnetic fabrics in the lower part (0–203 m), tectonism was mainly induced magnetically for the following observations. First, if magnetic fabrics were induced by currents, the magnetic lineations (K_{max}) generally covered a wider range of azimuths (Tarling and Hrouda, 1993). However, the three principal axes of magnetic fabrics in the lower part were well clustered, and the K_{min} axes exhibit a NE-SW girdle distribution, which is the typical feature of pencil structure magnetic fabrics that is commonly observed in foreland basin sediments along fold-and-thrust belts (Huang et al., 2006; Charreau et al., 2009; Tang et al., 2012; Yu et al., 2014; Tang et al., 2015; Li et al., 2020). Second, the magnetic lineations (K_{max}) were generally parallel to the bedding strikes, the Qigequan anticline axis and present-day GPS vectors in this region (Shen et al., 2001; Zhang et al., 2004; Zhang et al., 2007; Wang and Shen, 2020). Since the Qaidam Basin has been a compressional setting since the early Cenozoic as a result of the continuous N-S-ward continental collision between the Indian and Eurasian plates (Yin et al., 2008; Zhou et al., 2006; Wang et al., 2012; Wei et al., 2016; Bao et al., 2017), magnetic fabrics in the lower part were mostly attributed to the LPS process during deposition and can be used to trace the compressional strain conditions. The consistent NW-SE magnetic lineation (K_{max}, Dec = 306.1) and NE-SW girdle distribution of K_{min} axes indicate the constant NE-SW (~36.1°) compressional strain during this period.

Although the magnetic lineations were not well developed compared to the lower part with a broad NW-SE magnetic lineation (**Figures 3B,C**), the mean magnetic lineations of the middle (Dec = 307.1) and upper (Dec = 310.3) parts are consistent with that of the lower part, both of which are parallel to the bedding strikes. In addition, the K_{min} axes of the upper part also exhibit a broad NE-SW girdle distribution, suggesting possible NE-SW-ward compressional strain. Based on these observations, we believe these magnetic fabrics were still tectonism-induced results. However, the weak hydraulic force-induced fabrics cannot be totally ruled out, as the preferred orientation of magnetic lineations (~310°) was subparallel to the restored paleocurrent directions (~150°) (**Figure 2B**). But, the recent studies show that the magnetic fabric in the western Qaidam basin with strong tectonic deformation was easier to reveal the tectonic activity (Li et al., 2020; Li et al., 2021), which could be well correspond to the tectonic deformation found in the previous studies.

5.2 Prevalent NE-SW Compressional Strain in the Qaidam Basin Since the Late Miocene

In general, the strain directions are generally perpendicular to the magnetic lineations in the compressional settings (e.g., Borradaile and Henry, 1997; Soto et al., 2009; Li et al., 2020). Based on the observations that the mean magnetic lineation (NW-SE, ~127°) is generally parallel to the mean bedding strike (~123.7°)/fold axis and that the principal axes of K_{min} exhibit a girdle distribution, the characteristics of magnetic fabrics from the Qigequan profile are mostly attributed to LPS as a tectonic origin. Thus, the compressional strain direction in the Qigequan region in the late Neogene is NE (~36°). This direction is consistent with the results from the nearby Huatugou and Gansen regions, where NE-SW-ward compressional strain prevails during the deposition of the Xiaganchaigou and Xiayoushashan Fms (Li et al., 2008; Yu et al., 2014). These results together indicate that the compressional strain direction in the western Qaidam Basin possibly remains a constant NE-SW direction since at least the Late Eocene. This is quite different from that in the northern and middle Qaidam Basin with an obvious clockwise rotation from nearly N-S to NE-SW during the early Oligocene to late Miocene and Middle to Late Miocene, respectively (Li et al., 2020, 2021), indicating that these two regions possibly underwent different deformation processes as they were dominated by different geologic units (Yin et al., 2007; Yin et al., 2008). Nevertheless, the prevailing NE-SW compressional strain in the late Miocene in the western and northern Qaidam Basin is one of the key candidates to shape a series of NW-SE trending folds and faults within the Qaidam Basin that formed since the deposition of the Shangyoushashan Fm (~15 Ma), especially that of the Shizigou Fm (~8 Ma) (Mao et al., 2016; Li et al., 2017; Liu et al., 2019). This geological process would produce a relatively high topography in the western and northern Qaidam Basin and contribute to the southeastward propagation of the depocenter during the Cenozoic (Métivier et al., 1998; Wang et al., 2006; Yin et al., 2008; Yu et al., 2014).

5.3 Further Tectonic Implications of Anisotropy of Magnetic Susceptibility Parameters Variations

Most geologic activity records in and around the western Qaidam Basin, such as mountain buildings and thrusting, were mainly revealed by rapid cooling from thermochronology (Jolivet et al., 2001; Wang et al., 2006; Wang et al., 2008; Liu et al., 2017) or by growth strata from seismic reflection profiles (Wang et al., 2012; Cheng et al., 2014; Liu et al., 2019). These results generally have a large time scale and are sometimes insufficient to reveal detailed or late tectonic activities. Other successive records, such as abrupt changes in lithology, sedimentation rates and magnetic

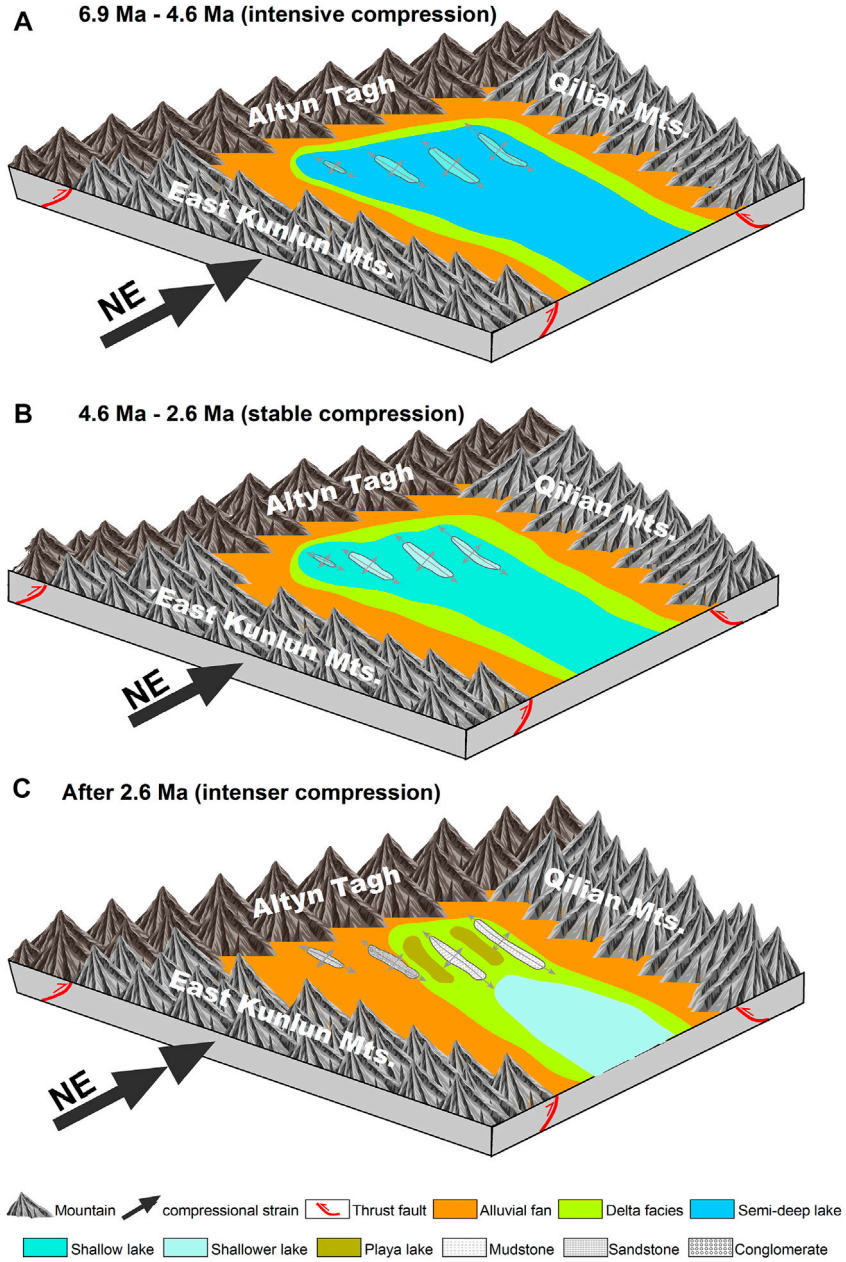

FIGURE 4 | Three tectonic stages inferred from the anisotropy of magnetic susceptibility (AMS) of the Qigequan profile illustrating the evolution of the lithofacies and the lake shrinking at the intense compressional stage between ~6.9 Ma and 4.6 Ma **(A)**, the stable compressional stage between 4.6 Ma and 2.6 Ma **(B)** and the relatively more intensive compressional stage after 2.6 Ma **(C)**.

susceptibility, are also quite related to climate change, and it is sometimes difficult to distinguish tectonic information from a single record (Fang et al., 2007; Chang et al., 2015; Zhang et al., 2016; Bao et al., 2017; Guan et al., 2019). The AMS parameters, especially Pj and T, which were both independent of lithology (**Figure 2**), provide deal proxies to track tectonic activities.

T is closely related to the tectonic strain, and it was mainly positive (oblate AMS ellipsoids) during deposition. With increasing strain, it becomes negative (prolate AMS ellipsoids; **Figure 3D**) and again returns to positive values (Parés et al., 1999; McCarthy et al., 2015). T exhibits an increasing trend from negative (prolate) to positive (oblate) in the lower part, while it remains positive throughout the middle and upper parts. Taken together with the distributions of the three principal axes (**Figure 3D**), the variations in T indicate an intense compressional strain with a weakening trend during ~6.9–4.6 Ma (**Figure 4A**). In addition, the proportion of prolate ellipsoids also shows a decreasing trend (from ~31 to 16%–9.8%) from bottom to top, suggesting plausible weakening tectonic deformation since ~6.9 Ma in the western Qaidam Basin.

Although the tectonic deformation during ~6.9–4.6 Ma slowly released the intense compressional strain in the Late Miocene; it did not transform the extent of the shallow lake and caused the eastward migration of the lake center, which resulted in the deposition of fine detritus in the anticline center (**Figure 4A**).

This weakening strain during ~6.9–4.6 Ma in the Qigequan anticline is first reported in the western Qaidam Basin. Many seismic reflection profiles have revealed the growth strata developed since the early Miocene in the areas southwest of the study region. The formation of the growth strata may be related to the activity of the Kunbei fault system (Yin et al., 2007; Yin et al., 2007; Cheng et al., 2014) since the middle Miocene (~15 Ma), especially the late Miocene (~8 Ma) east of the study region (Mao et al., 2016; Liu et al., 2019), suggesting intensive tectonic deformation since the early to late Miocene in the western Qaidam Basin. This is further supported by the middle-late Miocene mountain uplift revealed by apatite fission track analyses (Wang et al., 2008), vertical-axis block rotations (Li et al., 2017), abrupt increases in the sedimentation rate (Chang et al., 2015) and growth index of several faults (Wang et al., 2012) in the western Qaidam Basin. This early-late Miocene tectonic deformation possibly released most of the compressional strain since initiation, leading to decreasing tectonic strain during ~6.9–4.6 Ma.

Between 4.6 Ma and 2.6 Ma, T values are almost positive with an oblate magnetic fabric (**Figure 2**), and the K_{max} and K_{int} axes also have no obvious separation (**Figure 3C**), indicating a relatively weak and stable tectonic environment (**Figure 4B**). The crustal shortening rate in the basin center and the sedimentary accumulation and erosion rate in the basin margin revealed that the NE-SW compressional strain was still strong and successive (Zhou et al., 2006; Fang et al., 2007; Bao et al., 2017). The lithofacies with the dominate fine mudstone and siltstone intercalated conglomerate between 4.6 Ma and 2.6 Ma transformed from mudstone and calcareous mudstone between 6.9 Ma and 4.6 Ma (**Figure 2A**), hinting that the lake water level became shallower in the western Qaidam Basin and that the frontal region of mountains deposited coarser sediments (**Figure 4B**).

However, this is not the case for the upper part, where T values show no obvious change compared to the middle part (**Figure 2**). The unconformities (U_1) in the Qigequan region are direct evidence to reveal intensive tectonic activities at ~2.6 Ma (**Figure 2A**). More geological evidence has proposed that more intensive tectonic deformation has occurred since the deposition of the Qigequan Fm during the Quaternary. Restoration of balanced cross-sections all over the Qaidam Basin proved that the shortening rate of the upper crust or sediment flux increased several times compared to the averaged values (Zhou et al., 2006; Wei et al., 2016; Bao et al., 2017). In addition, a rapid increase in the sediment accumulation rate at ~2.6–2.2 Ma was also reported from drilling cores by magnetostratigraphic studies in the western Qaidam Basin (Zhang et al., 2012; Zhang et al., 2020b). The more intensive NE-SW compressional strain after 2.6 Ma brought about crustal shortening, the onset of the depocenter shifted eastward, the shallow lake shrank and the emergence of playa lakes (**Figure 4C**). The basin margins and even the anticline center started to deposit conglomerates, and the range of alluvial fans began to expand after 2.6 Ma (**Figure 4C**), and the basin depocenter ultimately withdrew from the western Qaidam Basin at 0.1 Ma (Zhang et al., 2020b). Thus, the ~2.6 Ma tectonic deformation is quite intensive and popular in the western Qaidam Basin. However, this geological event is not reflected by the AMS parameters (T).

Previous studies that used AMS to reflect deformation information were mainly based on fine-grained mudstones (Parés et al., 1999; Soto et al., 2009). Compared to the lower and middle, the upper part is mainly composed of sandstone and sandy conglomerate (**Figure 2A**). These rocks generally have fewer magnetic, phyllosilicate or clay minerals. In addition, coarse grains are more likely to be influenced by gravity and hydraulic forces. All these factors indicate that the AMS results in coarse-grained lithology are inappropriate to reflect the geological process during deposition.

6 CONCLUSION

A successive AMS record since the Late Neogene has been collected along the ~800-m-thick Qigequan profile in the western Qaidam Basin. The magnetic lineations were generally parallel to the bedding strikes. Based on the distributions of AMS parameters and three principal axes, the AMS data can be divided into three parts. The lower part with well-clustered magnetic lineation and NE-SW girdle distribution of K_{min} indicate tectonism-induced magnetic fabrics and suggest a constant NE-SW compressional strain direction. We believe that the magnetic fabric along the entire profile was influenced by a NE-SW compression. However, weak hydraulic force-induced fabrics cannot be totally ruled out, as the restored paleocurrent directions were subparallel to the magnetic lineations.

NE-SW compressional strain has been prevalent in the western Qaidam Basin since at least the Late Miocene and could contribute to the southeastward migration of the depocenter of the Qaidam Basin in the Cenozoic. In addition, T revealed the change in the intensity of the deformation since 4.6 Ma, as most of the compressional strain was released during the early-late Miocene initiation of tectonic deformation in the western Qaidam Basin. Furthermore, the inconsistent relations between the AMS parameters and intensive deformation during the deposition of the upper part (~2.6 Ma) suggest that the coarse-grained lithology is inappropriate to reflect the geological process during deposition.

DATA AVAILABILITY STATEMENT

The datasets presented in this study can be found in online repositories. The names of the repository/repositories and accession number(s) can be found below: https://doi.org/10.6084/m9.figshare.17310626.v1.

AUTHOR CONTRIBUTIONS

WZ: Conceptualization, writing–review and editing, and investigation. BL: Formal analysis, investigation, and measurement. MY: Investigation, resources, and supervision.

FUNDING

This work was cosupported by the National Natural Science Foundation of China (41672358, 41804065, 41974080, and 41620104002), the Strategic Priority Research Program of the Chinese Academy of Sciences (XDA20070201), the Second Tibetan Plateau Scientific Expedition and Research Program (STEP) (2019QZKK0707), the National Basic Research Program of China (grant 2017YFC0602803), and the External Cooperation Program (Grant 131C11KYSB20160072).

ACKNOWLEDGMENTS

We thank Long Xiaoyong, Gao Hongshan, Sun Ranhao, Zhao Yande, Dai Shuang, Gao Donglin, Xu Xianhai and Li Lili for field and laboratory assistance.

REFERENCES

Bao, J., Wang, Y., Song, C., Feng, Y., Hu, C., Zhong, S., et al. (2017). Cenozoic Sediment Flux in the Qaidam Basin, Northern Tibetan Plateau, and Implications with Regional Tectonics and Climate. *Glob. Planet. Change* 155, 56–69. doi:10.1016/j.gloplacha.2017.03.006

Borradaile, G. J., and Henry, B. (1997). Tectonic Applications of Magnetic Susceptibility and its Anisotropy. *Earth-Science Rev.* 42, 49–93. doi:10.1016/S0012-8252(96)00044-X

Chang, H., Li, L., Qiang, X., Garzione, C. N., Pullen, A., and An, Z. (2015). Magnetostratigraphy of Cenozoic Deposits in the Western Qaidam Basin and its Implication for the Surface Uplift of the Northeastern Margin of the Tibetan Plateau. *Earth Planet. Sci. Lett.* 430, 271–283. doi:10.1016/j.epsl.2015.08.029

Charreau, J., Chen, Y., Gilder, S., Barrier, L., Dominguez, S., Augier, R., et al. (2009). Neogene Uplift of the Tian Shan Mountains Observed in the Magnetic Record of the Jingou River Section (Northwest China). *Tectonics* 28, 224–243. doi:10.1029/2007TC002137

Chen, C., Bai, Y., Fang, X., Xu, Q., Zhang, T., Deng, T., et al. (2020). Lower-altitude of the Himalayas before the Mid-pliocene as Constrained by Hydrological and thermal Conditions. *Earth Planet. Sci. Lett.* 545, 116422. doi:10.1016/j.epsl.2020.116422

Chen, Y., Yan, M., Fang, X., Song, C., Zhang, W., Zan, J., et al. (2017). Detrital Zircon U-Pb Geochronological and Sedimentological Study of the Simao Basin, Yunnan: Implications for the Early Cenozoic Evolution of the Red River. *Earth Planet. Sci. Lett.* 476, 22–33. doi:10.1016/j.epsl.2017.07.025

Cheng, F., Garzione, C., Jolivet, M., Guo, Z., Zhang, D., and Zhang, C. (2018). A New Sediment Accumulation Model of Cenozoic Depositional Ages from the Qaidam basin, Tibetan Plateau. *J. Geophys. Res. Earth Surf.* 123 (11), 3101–3121. doi:10.1029/2018JF004645

Cheng, F., Jolivet, M., Fu, S., Zhang, Q., Guan, S., Yu, X., et al. (2014). Northward Growth of the Qimen Tagh Range: A New Model Accounting for the Late Neogene Strike-Slip Deformation of the SW Qaidam Basin. *Tectonophysics* 632, 32–47. doi:10.1016/j.tecto.2014.05.034

Fang, X., An, Z., Clemens, S. C., Zan, J., Shi, Z., Yang, S., et al. (2020a). The 3.6-Ma Aridity and Westerlies History over Midlatitude Asia Linked with Global Climatic Cooling. *Proc. Natl. Acad. Sci. USA.* 117 (40), 24729–24734. doi:10.1073/pnas.1922710117

Fang, X., Dupont-Nivet, G., Wang, C., Song, C., Meng, Q., Zhang, W., et al. (2020b). Revised Chronology of central Tibet Uplift (Lunpola Basin). *Sci. Adv.* 6, eaba7298. doi:10.1126/sciadv.aba7298

Fang, X., Galy, A., Yang, Y., Zhang, W., Ye, C., and Song, C. (2019). Paleogene Global Cooling-Induced Temperature Feedback on Chemical Weathering, as Recorded in the Northern Tibetan Plateau. *Geology* 47, 992–996. doi:10.1130/G46422.1

Fang, X., Zhang, W., Meng, Q., Gao, J., Wang, X., King, J., et al. (2007). High-resolution Magnetostratigraphy of the Neogene Huaitoutala Section in the Eastern Qaidam Basin on the NE Tibetan Plateau, Qinghai Province, China and its Implication on Tectonic Uplift of the NE Tibetan Plateau. *Earth Planet. Sci. Lett.* 258, 293–306. doi:10.1016/j.epsl.2007.03.042

Guan, C., Chang, H., Yan, M., Li, L., Xia, M., Zan, J., et al. (2019). Rock Magnetic Constraints for the Mid-miocene Climatic Optimum from a High-Resolution Sedimentary Sequence of the Northwestern Qaidam Basin, NE Tibetan Plateau. *Palaeogeogr. Palaeoclimatol. Palaeoecol.* 532, 109263. doi:10.1016/j.palaeo.2019.109263

Holt, W. E., Chamot-Rooke, N., Le Pichon, X., Haines, A. J., Shen-Tu, B., and Ren, J. (2000). Velocity Field in Asia Inferred from Quaternary Fault Slip Rates and Global Positioning System Observations. *J. Geophys. Res.* 105, 19185–19209. doi:10.1029/2000JB900045

Hrouda, F. e. (1982). Magnetic Anisotropy of Rocks and its Application in Geology and Geophysics. *Geophys. Surv.* 5, 37–82. doi:10.1007/BF01450244

Huang, B., Piper, J., Peng, S., Liu, T., Li, Z., Wang, Q., et al. (2006). Magnetostratigraphic Study of the Kuche Depression, Tarim Basin, and Cenozoic Uplift of the Tian Shan Range, Western China. *Earth Planet. Sci. Lett.* 251, 346–364. doi:10.1016/j.epsl.2006.09.020

Huo, F., Shao, R., Jiang, N., Zhang, R., Cheng, X., Wei, B., et al. (2020). Anisotropy of Magnetic Susceptibility of Mesozoic and Cenozoic Sediments in the Northern Margin of Qaidam Basin and its Sedimentary-Tectonic Significance. *Chin. J. Geophys. (In Chinese)* 63, 583–596. doi:10.6038/cjg2020N0038

Ji, J., Zhang, K., Clift, P. D., Zhuang, G., Song, B., Ke, X., et al. (2017). High-resolution Magnetostratigraphic Study of the Paleogene-Neogene Strata in the Northern Qaidam Basin: Implications for the Growth of the Northeastern Tibetan Plateau. *Gondwana Res.* 46, 141–155. doi:10.1016/j.gr.2017.02.015

Jolivet, M., Brunel, M., Seward, D., Xu, Z., Yang, J., Roger, F., et al. (2001). Mesozoic and Cenozoic Tectonics of the Northern Edge of the Tibetan Plateau: Fission-Track Constraints. *Tectonophysics* 343, 111–134. doi:10.1016/S0040-1951(01)00196-2

Larrasoaña, J. C., Gómez-Paccard, M., Giralt, S., and Roberts, A. P. (2011). Rapid Locking of Tectonic Magnetic Fabrics in Weakly Deformed Mudrocks. *Tectonophysics* 507, 16–25. doi:10.1016/j.tecto.2011.05.003

Larrasoaña, J. C., Pueyo, E. L., and Parés, J. M. (2004). An Integrated AMS, Structural, Palaeo- and Rock-Magnetic Study of Eocene marine Marls from the Jaca-Pamplona basin (Pyrenees, N Spain); New Insights into the Timing of Magnetic Fabric Acquisition in Weakly Deformed Mudrocks. *Geol. Soc. Lond. Spec. Publications* 238, 127–143. doi:10.1144/GSL.SP.2004.238.01.10

Li, B., Yan, M., Zhang, W., Fang, X., Meng, Q., Zan, J., et al. (2017). New Paleomagnetic Constraints on Middle Miocene Strike-Slip Faulting along the Middle Altyn Tagh Fault. *J. Geophys. Res. Solid Earth* 122, 4106–4122. doi:10.1002/2017JB014058

Li, B., Yan, M., Zhang, W., Fang, X., Yang, Y., Zhang, D., et al. (2018). Paleomagnetic Rotation Constraints on the Deformation of the Northern Qaidam Marginal Thrust Belt and Implications for Strike-Slip Faulting along the Altyn Tagh Fault. *J. Geophys. Res. Solid Earth* 123, 7207–7224. doi:10.1029/2018JB015753

Li, B., Yan, M., Zhang, W., Fang, X., Yang, Y., Zhang, D., et al. (2021). Two-stage Strike-Slip Faulting of the Altyn Tagh Fault Revealed by Magnetic Fabrics in the Qaidam Basin. *Tectonophysics* 821, 229142. doi:10.1016/j.tecto.2021.229142

Li, B., Yan, M., Zhang, W., Parés, J. M., Fang, X., Yang, Y., et al. (2020). Magnetic Fabric Constraints on the Cenozoic Compressional Strain Changes in the Northern Qaidam Marginal Thrust Belt and Their Tectonic Implications. *Tectonics* 39, e2019TC005989. doi:10.1029/2019TC005989

Li, L., Guo, Z., Guan, S., Zhou, S., Wang, M., Fang, Y., et al. (2015). Heavy mineral Assemblage Characteristics and the Cenozoic Paleogeographic Evolution in

Southwestern Qaidam Basin. *Sci. China Earth Sci.* 58, 859–875. doi:10.1007/s11430-014-5050-x

Li, L., Ren, X., Jiang, R., Qi, W., Wu, Y., Yang, Q., et al. (2008). Magnetic Fabrics of Cenozoic Sedimentary Rocks in the Western Qaidam Basin and Their Shtuctural Significance. *J. Geomech.* 14, 45–56. doi:10.3969/j.issn.1006-6616.2008.01.004

Liu, D., Li, H., Sun, Z., Pan, J., Wang, M., Wang, H., et al. (2017). AFT Dating Constrains the Cenozoic Uplift of the Qimen Tagh Mountains, Northeast Tibetan Plateau, Comparison with LA-ICPMS Zircon U-Pb Ages. *Gondwana Res.* 41, 438–450. doi:10.1016/j.gr.2015.10.008

Liu, R., Chen, Y., Yu, X., Du, W., Cheng, X., and Guo, Z. (2019). An Analysis of Distributed Strike-Slip Shear Deformation of the Qaidam Basin, Northern Tibetan Plateau. *Geophys. Res. Lett.* 46, 4202–4211. doi:10.1029/2018GL081523

Lu, H., and Xiong, S. (2009). Magnetostratigraphy of the Dahonggou Section, Northern Qaidam Basin and its Bearing on Cenozoic Tectonic Evolution of the Qilian Shan and Altyn Tagh Fault. *Earth Planet. Sci. Lett.* 288, 539–550. doi:10.1016/j.epsl.2009.10.016

Macdonald, W. D., and Palmer, H. C. (1990). Flow Directions in Ash-Flow Tuffs: a Comparison of Geological and Magnetic Susceptibility Measurements, Tshirege Member (Upper Bandelier Tuff), Valles Caldera, New Mexico, USA. *Bull. Volcanol.* 53, 45–59. doi:10.1007/BF00680319

Maher, B. A., and Thompson, R. (1992). Paleoclimatic Significance of the mineral Magnetic Record of the Chinese Loess and Paleosols. *Quat. Res.* 37, 155–170. doi:10.1016/0033-5894(92)90079-X

Mao, L., Xiao, A., Zhang, H., Wu, Z., Wang, L., Shen, Y., et al. (2016). Structural Deformation Pattern within the NW Qaidam Basin in the Cenozoic Era and its Tectonic Implications. *Tectonophysics* 687, 78–93. doi:10.1016/j.tecto.2016.09.008

Martin, C., and Jelinek, V. (2009). *Anisoft 4.2: Anisotropy Data Browser for Windows*. Agico Inc: Brno, Czech Republic.

Mccarthy, D. J., Meere, P. A., and Petronis, M. S. (2015). A Comparison of the Effectiveness of Clast Based Finite Strain Analysis Techniques to AMS in Sandstones from the Sevier Thrust Belt, Wyoming. *Tectonophysics* 639, 68–81. doi:10.1016/j.tecto.2014.11.014

Métivier, F., Gaudemer, Y., Tapponnier, P., and Meyer, B. (1998). Northeastward Growth of the Tibet Plateau Deduced from Balanced Reconstruction of Two Depositional Areas: The Qaidam and Hexi Corridor Basins, China. *Tectonics* 17, 823–842. doi:10.1029/98TC02764

Nie, J., Ren, X., Saylor, J. E., Su, Q., Horton, B. K., Bush, M. A., et al. (2019). Magnetic Polarity Stratigraphy, Provenance, and Paleoclimate Analysis of Cenozoic Strata in the Qaidam Basin, NE Tibetan Plateau. *Geol. Soc. Am. Bull.* 132, 310–320. doi:10.1130/B35175.1

Parés, J. M., Ben, V. D. P., and Dinarès, J. (1999). Evolution of Magnetic Fabrics during Incipient Deformation of Mudrocks (Pyrenees, Northern Spain). *Tectonophysics* 307, 1–14. doi:10.1016/S0040-1951(99)00115-8

Pueyo Anchuela, Ó., Pueyo, E. L., Pocoví Juan, A., and Gil Imaz, A. (2012). Vertical axis Rotations in Fold and Thrust Belts: Comparison of AMS and Paleomagnetic Data in the Western External Sierras (Southern Pyrenees). *Tectonophysics* 532-535, 119–133. doi:10.1016/j.tecto.2012.01.023

Qinghai, B. G. M. R. (1991). *Regional Geology of Qinghai Province*. Beijing: Geological Publishing House.

Shen, Z.-K., Wang, M., Li, Y., Jackson, D. D., Yin, A., Dong, D., et al. (2001). Crustal Deformation along the Altyn Tagh Fault System, Western China, from GPS. *J. Geophys. Res.* 106, 30607–30621. doi:10.1029/2001JB000349

Song, C., Hu, S., Han, W., Zhang, T., Fang, X., Gao, J., et al. (2014). Middle Miocene to Earliest Pliocene Sedimentological and Geochemical Records of Climate Change in the Western Qaidam Basin on the NE Tibetan Plateau. *Palaeogeogr. Palaeoclimatol. Palaeoecol.* 395, 67–76. doi:10.1016/j.palaeo.2013.12.022

Soto, R., Larrasoaña, J. C., Arlegui, L. E., Beamud, E., Oliva-Urcia, B., and Simón, J. L. (2009). Reliability of Magnetic Fabric of Weakly Deformed Mudrocks as a Palaeostress Indicator in Compressive Settings. *J. Struct. Geology.* 31, 512–522. doi:10.1016/j.jsg.2009.03.006

Su, Q., Nie, J., Saylor, J. E., Horton, B. K., Bush, M. A., and Chen, W. (2016). An Anisotropy of Magnetic Susceptibility Study of the Cenozoic Dahonggou Section in Northern Qaidam Basin and its Tectonic Implications. *Quat. Sci.* 36, 859–869. doi:10.11928/j.issn.1001-7410.2016.04.07

Sun, J., Xiao, W., Windley, B. F., Ji, W., Fu, B., Wang, J., et al. (2016). Provenance Change of Sediment Input in the Northeastern Foreland of Pamir Related to Collision of the Indian Plate with the Kohistan-Ladakh Arc at Around 47 Ma. *Tectonics* 35, 315–338. doi:10.1002/2015TC003974

Sun, J., Zhu, R., and An, Z. (2005a). Tectonic Uplift in the Northern Tibetan Plateau since 13.7 Ma Ago Inferred from Molasse Deposits along the Altyn Tagh Fault. *Earth Planet. Sci. Lett.* 235, 641–653. doi:10.1016/j.epsl.2005.04.034

Sun, Z., Yang, Z., Pei, J., Ge, X., Wang, X., Yang, T., et al. (2005b). Magnetostratigraphy of Paleogene Sediments from Northern Qaidam Basin, China: Implications for Tectonic Uplift and Block Rotation in Northern Tibetan Plateau. *Earth Planet. Sci. Lett.* 237, 635–646. doi:10.1016/j.epsl.2005.07.007

Tang, Z., Dong, X., Wang, X., and Ding, Z. (2015). Oligocene-Miocene Magnetostratigraphy and Magnetic Anisotropy of theBaxbulak Section from thePamir-TianShan Convergence Zone. *Geochem. Geophys. Geosyst.* 16, 3575–3592. doi:10.1002/2015GC005965

Tang, Z., Huang, B., Dong, X., Ji, J., and Ding, Z. (2012). Anisotropy of Magnetic Susceptibility of the Jingou River Section: Implications for Late Cenozoic Uplift of the Tian Shan. *Geochem. Geophys. Geosyst.* 13, 487–497. doi:10.1029/2011gc003966

Tapponnier, P., and Molnar, P. (1977). Active Faulting and Tectonics in China. *J. Geophys. Res.* 82, 2905–2930. doi:10.1029/2011GC00396610.1029/jb082i020p02905

Tarling, D., and Hrouda, F. (1993). *Magnetic Anisotropy of Rocks*. London: Chapman & Hall.

Thompson, R., Stober, J. C., Turner, G. M., Oldfield, F., Bloemendal, J., Dearing, J. A., et al. (1980). Environmental Applications of Magnetic Measurements. *Science* 207, 481–486. doi:10.1126/science.207.4430.481

Tian, X., Bai, Z., Klemperer, S. L., Liang, X., Liu, Z., Wang, X., et al. (2021). Crustal-scale Wedge Tectonics at the Narrow Boundary between the Tibetan Plateau and Ordos Block. *Earth Planet. Sci. Lett.* 554, 116700. doi:10.1016/j.epsl.2020.116700

Wang, E., Xu, F.-Y., Zhou, J.-X., Wan, J., and Burchfiel, B. C. (2006). Eastward Migration of the Qaidam basin and its Implications for Cenozoic Evolution of the Altyn Tagh Fault and Associated River Systems. *Geol. Soc. America Bull.* 118, 349–365. doi:10.1130/B25778.1

Wang, M., and Shen, Z. K. (2020). Present-Day Crustal Deformation of Continental China Derived from GPS and its Tectonic Implications. *J. Geophys. Res. Solid Earth* 125 (2), 18774. doi:10.1029/2019JB018774

Wang, S., Ma, C., She, Z., Chen, Z., and Yang, Y. (2008). Apatite Fission Track Analyses of Cenozoic Sedimentary Source and Basin Thermal History in West Qaidam Basin. *Geol. Sci. Technol. Inform.* 27, 30–36. doi:10.3969/j.issn.1000-7849.2008.05.005

Wang, W., Zheng, W., Zhang, P., Li, Q., Kirby, E., Yuan, D., et al. (2017). Expansion of the Tibetan Plateau during the Neogene. *Nat. Commun.* 8, 15887. doi:10.1038/ncomms15887

Wang, Y., Zheng, J., Zhang, W., Li, S., Liu, X., Yang, X., et al. (2012). Cenozoic Uplift of the Tibetan Plateau: Evidence from the Tectonic-Sedimentary Evolution of the Western Qaidam Basin. *Geosci. Front.* 3, 175–187. doi:10.1016/j.gsf.2011.11.005

Wei, Y., Xiao, A., Wu, L., Mao, L., Zhao, H., Shen, Y., et al. (2016). Temporal and Spatial Patterns of Cenozoic Deformation across the Qaidam Basin, Northern Tibetan Plateau. *Terra Nova* 28, 409–418. doi:10.1111/ter.12234

Weil, A. B., and Yonkee, A. (2009). Anisotropy of Magnetic Susceptibility in Weakly Deformed Red Beds from the Wyoming Salient, Sevier Thrust belt: Relations to Layer-Parallel Shortening and Orogenic Curvature. *Lithosphere* 1 (4), 235–256. doi:10.1130/l42.1

Wu, L., Xiao, A., Wang, L., Mao, L., Wang, L., Dong, Y., et al. (2012). EW-trending Uplifts along the Southern Side of the central Segment of the Altyn Tagh Fault, NW China: Insight into the Rising Mechanism of the Altyn Mountain during the Cenozoic. *Sci. China Earth Sci.* 55, 926–939. doi:10.1007/s11430-012-4402-7

Xiong, Z., Ding, L., Spicer, R. A., Farnsworth, A., Wang, X., Valdes, P. J., et al. (2020). The Early Eocene Rise of the Gonjo Basin, SE Tibet: From Low Desert to High forest. *Earth Planet. Sci. Lett.* 543, 116312. doi:10.1016/j.epsl.2020.116312

Yin, A., Dang, Y.-Q., Wang, L.-C., Jiang, W.-M., Zhou, S.-P., Chen, X.-H., et al. (2008). Cenozoic Tectonic Evolution of Qaidam basin and its Surrounding Regions (Part 1): The Southern Qilian Shan-Nan Shan Thrust belt and Northern Qaidam basin. *Geol. Soc. America Bull.* 120, 813–846. doi:10.1130/b26180.1

Yin, A., Dang, Y., Zhang, M., McRivette, M. W., Burgess, W. P., and Chen, X. (2007). Cenozoic Tectonic Evolution of Qaidam basin and its Surrounding Regions (Part 2): Wedge Tectonics in Southern Qaidam basin and the Eastern Kunlun Range. *Geol. Soc. Am. Bull.* 433, 369–390. doi:10.1130/2007.2433(18)

Yin, A., and Harrison, T. M. (2000). Geologic Evolution of the Himalayan-Tibetan Orogen. *Annu. Rev. Earth Planet. Sci.* 28, 211–280. doi:10.1146/annurev.earth.28.1.211

Yin, A., Nie, S., Craig, P., Harrison, T. M., Ryerson, F. J., Xianglin, Q., et al. (1998). Late Cenozoic Tectonic Evolution of the Southern Chinese Tian Shan. *Tectonics* 17, 1–27. doi:10.1029/97TC03140

Yin, A., Rumelhart, P. E., Butler, R., Cowgill, E., Harrison, T. M., Foster, D. A., et al. (2002). Tectonic History of the Altyn Tagh Fault System in Northern Tibet Inferred from Cenozoic Sedimentation. *Geol. Soc. Am. Bull.* 114, 1257–1295. doi:10.1130/0016-7606(2002)114<1257:thotat>2.0.co;2

Yu, X., Huang, B., Guan, S., Fu, S., Cheng, F., Cheng, X., et al. (2014). Anisotropy of Magnetic Susceptibility of Eocene and Miocene Sediments in the Qaidam Basin, Northwest China: Implication for Cenozoic Tectonic Transition and Depocenter Migration. *Geochem. Geophys. Geosyst.* 15, 2095–2108. doi:10.1002/2014GC005231

Zhang, P.-Z., Molnar, P., and Xu, X. (2007). Late Quaternary and Present-Day Rates of Slip along the Altyn Tagh Fault, Northern Margin of the Tibetan Plateau. *Tectonics* 26, 1–8. doi:10.1029/2006TC002014

Zhang, P.-Z., Shen, Z., Wang, M., Gan, W., Bürgmann, R., Molnar, P., et al. (2004). Continuous Deformation of the Tibetan Plateau from Global Positioning System Data. *Geol* 32, 809–812. doi:10.1130/G20554.1

Zhang, R., Kravchinsky, V. A., Zhu, R., and Yue, L. (2010). Paleomonsoon Route Reconstruction along a W-E Transect in the Chinese Loess Plateau Using the Anisotropy of Magnetic Susceptibility: Summer Monsoon Model. *Earth Planet. Sci. Lett.* 299, 436–446. doi:10.1016/j.epsl.2010.09.026

Zhang, T., Han, W., Fang, X., Zhang, W., Song, C., and Yan, M. (2016). Intensified Tectonic Deformation and Uplift of the Altyn Tagh Range Recorded by Rock Magnetism and Growth Strata Studies of the Western Qaidam Basin, NE Tibetan Plateau. *Glob. Planet. Change* 137, 54–68. doi:10.1016/j.gloplacha.2015.12.017

Zhang, W., Appel, E., Fang, X., Setzer, F., Song, C. H., Meng, Q. Q., et al. (2020b). New Paleomagnetic Constraints on Syntectonic Growth Strata in the Western Qaidam Basin, NE Tibetan Plateau. *Tectonophysics* 780, 228401. doi:10.1016/j.tecto.2020.228401

Zhang, W., Appel, E., Fang, X., Song, C., and Cirpka, O. (2012). Magnetostratigraphy of Deep Drilling Core SG-1 in the Western Qaidam Basin (NE Tibetan Plateau) and its Tectonic Implications. *Quat. Res.* 78, 139–148. doi:10.1016/j.yqres.2012.03.011

Zhang, W., Fang, X., Song, C., Appel, E., Yan, M., and Wang, Y. (2013). Late Neogene Magnetostratigraphy in the Western Qaidam Basin (NE Tibetan Plateau) and its Constraints on Active Tectonic Uplift and Progressive Evolution of Growth Strata. *Tectonophysics* 599, 107–116. doi:10.1016/j.tecto.2013.04.010

Zhang, W., Fang, X., Zhang, T., Song, C., and Yan, M. (2020a). Eocene Rotation of the Northeastern Central Tibetan Plateau Indicating Stepwise Compressions and Eastward Extrusions. *Geophys. Res. Lett.* 47, e2020GL088989. doi:10.1029/2020GL088989

Zhou, J., Xu, F., Wang, T., Cao, A., and Yin, C. (2006). Cenozoic Deformation History of the Qaidam Basin, NW China: Results from Cross-Section Restoration and Implications for Qinghai-Tibet Plateau Tectonics. *Earth Planet. Sci. Lett.* 243, 195–210. doi:10.1016/j.epsl.2005.11.033

Zhou, L. P., Oldfield, F., Wintle, A. G., Robinson, S. G., and Wang, J. T. (1990). Partly Pedogenic Origin of Magnetic Variations in Chinese Loess. *Nature* 346, 737–739. doi:10.1038/346737a0

Conflict of Interest: The authors declare that the research was conducted in the absence of any commercial or financial relationships that could be construed as a potential conflict of interest.